



Contents lists available at ScienceDirect

Biochemical and Biophysical Research Communications

journal homepage: [www.elsevier.com/locate/ybbrc](http://www.elsevier.com/locate/ybbrc)

## Temperature-induced labelling of Fluo-3 AM selectively yields brighter nucleus in adherent cells



Guixian Meng<sup>a</sup>, Leitong Pan<sup>a,\*</sup>, Cunbo Li<sup>a</sup>, Fen Hu<sup>a</sup>, Xuechen Shi<sup>a</sup>, Imshik Lee<sup>a</sup>, Irena Drevenšek-Olenik<sup>b</sup>, Xinzheng Zhang<sup>a</sup>, Jingjun Xu<sup>a</sup>

<sup>a</sup>The Key Laboratory of Weak-Light Nonlinear Photonics, Ministry of Education, School of Physics and TEDA Applied Physics Institute, Nankai University, Tianjin, China

<sup>b</sup>Faculty of Mathematics and Physics, University of Ljubljana, and J. Stefan Institute, Ljubljana, Slovenia

### ARTICLE INFO

#### Article history:

Received 3 December 2013

Available online 28 December 2013

#### Keywords:

Calcium imaging

Fluo-3 AM

Temperature

Brighter nucleus

Adherent cells

### ABSTRACT

Fluo-3 is widely used to study cell calcium. Two traditional approaches: (1) direct injection and (2) Fluo-3 acetoxyethyl ester (AM) loading, often bring conflicting results in cytoplasmic calcium ( $[Ca^{2+}]_c$ ) and nuclear calcium ( $[Ca^{2+}]_n$ ) imaging. AM loading usually yields a darker nucleus than in cytoplasm, while direct injection always induces a brighter nucleus which is more responsive to  $[Ca^{2+}]_n$  detection. In this work, we detailedly investigated the effects of loading and de-esterification temperatures on the fluorescence intensity of Fluo-3 in response to  $[Ca^{2+}]_n$  and  $[Ca^{2+}]_c$  in adherent cells, including osteoblast, HeLa and BV2 cells. Interestingly, it showed that fluorescence intensity of nucleus in osteoblast cells was about two times larger than that of cytoplasm when cells were loaded with Fluo-3 AM at 4 °C and allowed a subsequent step for de-esterification at 20 °C. Brighter nuclei were also acquired in HeLa and BV2 cells using the same experimental condition. Furthermore, loading time and adhesion quality of cells had effect on fluorescence intensity. Taken together, cold loading and room temperature de-esterification treatment of Fluo-3 AM selectively yielded brighter nucleus in adherent cells.

© 2013 Elsevier Inc. All rights reserved.

### 1. Introduction

$Ca^{2+}$  is an important intracellular messenger that regulates a variety of cellular functions, including those performed in the cell nucleus. It was reported that modifications of gene expression could be triggered by cytoplasmic calcium concentration ( $[Ca^{2+}]_c$ ) as well as by nuclear calcium concentration ( $[Ca^{2+}]_n$ ) [1]. Most of the research work performed in this field was focused on investigations of  $[Ca^{2+}]_c$ -related effects. However, in the recent two decades, effects related to  $[Ca^{2+}]_n$  have attracted increasing attentions. It is proposed that  $[Ca^{2+}]_n$  regulates gene expression more directly and efficiently than that of  $[Ca^{2+}]_c$  [2–5]. For instance,  $[Ca^{2+}]_n$  can result in gene transcription via NAFT (the nuclear factor of activated T cells) family of proteins [2] or DREAM (the downstream regulatory element antagonist modulator) [3]. In addition, several lines of evidence suggest that  $Ca^{2+}$  signaling in the nucleus and in the cytoplasm usually take place independently from each other [3,6], such as uncoupled  $[Ca^{2+}]_c$  and  $[Ca^{2+}]_n$  signals induced by histamine in HeLa cells [3] and by ATP in HepG<sub>2</sub> cells [6].

To investigate specific features related to  $[Ca^{2+}]_c$  and  $[Ca^{2+}]_n$ , it is essential to perform an accurate and reliable monitoring of the  $Ca^{2+}$  concentration in the two cell compartments simultaneously.

\* Corresponding author. Fax: +86 22 66229310.

E-mail address: [plt@nankai.edu.cn](mailto:plt@nankai.edu.cn) (L. Pan).

In most studies of this kind,  $Ca^{2+}$ -sensitive fluorescence indicators are used. Nevertheless, there exist several controversies when using fluorescent probes to measure  $[Ca^{2+}]_c$  and  $[Ca^{2+}]_n$ . O'Malley et al. reported conflicting results obtained by two conventional loading methods, namely direct injection and membrane-permeant acetoxyethyl ester (AM) loading [7]. The former invariably induced brighter fluorescence in the nucleus than in the cytoplasm, while the latter usually gave an opposite result. This behavior was observed for Indo-1 and Fura-2, as well as Fluo-3 indicators [8–11]. Additionally, it was found that measurements gave inconsistent results for AM-modified indicators loaded at different temperatures. Room temperature staining tended to result in a little brighter nucleus whereas warm temperature (37 °C) often gave darker nucleus [8,11]. These inconsistent indications could mislead investigators and drive them to wrong conclusions.

Despite the fact that direct injection usually gives more consistent results than the use of AM-modified indicators, one should not overlook its disadvantages, such as cell damage, long-lasting procedure, and operating complexity [12]. For these reasons, AM-modified indicators have recently found widespread applications in fluorescent imaging and Fluo-3 AM is at present regarded as one of the most suitable indicators for the detection of  $[Ca^{2+}]_c$  [13–15]. For evaluating this method, the goal of our study was to study the effects of loading and de-esterification temperatures on the fluorescence intensity of Fluo-3 AM in response to nuclear

and cytoplasmic calcium in osteoblast, HeLa and BV2 cells, respectively. On the basis of the obtained results, we developed a novel method to yield brighter fluorescence in the nucleus than in cytoplasm.

## 2. Materials and methods

### 2.1. Cell cultures

Osteoblast cells were prepared and cultured as described in our earlier work [16]. HeLa cells were obtained from the Key Laboratory of Bioactive Materials and BV2 cells from School of Physics, both at Nankai University in Tianjin, China. All cells grew in DMEM medium (Gibco, USA), including 15% FBS (Lanzhou National Hyclone Bio-engineering Co., Ltd., China) and 100 U penicillin + 100 µg/mL streptomycin (Gibco, USA). They were cultured at 37 °C in MCO175 incubator (SANYO Electric Biomedical Co., Japan) with 5% CO<sub>2</sub>. Before experiments, cells were incubated on glass cover slips and returned to the incubator for 24 h to ensure adequate adhesion.

### 2.2. Fluo-3 AM staining

Stock solutions (5 mM) of Fluo-3 AM (Invitrogen Co., USA) were prepared by using a solution of 20% (w/v) Pluronic F-127 in absolute dimethylsulphoxide. The aliquots were diluted with Hanks balanced salt solution (HBSS) (0.39 g/L KCl, 0.07 g/L KH<sub>2</sub>PO<sub>4</sub>, 8.06 g/L NaCl, 0.10 g/L Na<sub>2</sub>HPO<sub>4</sub>·7H<sub>2</sub>O, 0.24 g/L CaCl<sub>2</sub>, 0.10 g/L MgCl<sub>2</sub>, 0.10 g/L MgSO<sub>4</sub>, and 1.52 g/L D-glucose) to give the final concentrations of 5 µM.

The entire staining procession of Fluo-3 AM involves two stages: loading and de-esterification. The investigated cells were loaded with 5 µM Fluo-3 AM at  $T_L = 4, 20$  and 37 °C ( $T_L$ : loading temperature), respectively. Then, they were washed in pure HBSS and left for a further 30 min at  $T_D = 20$  or 37 °C to allow de-esterification ( $T_D$ : de-esterification temperature).

### 2.3. Microscopy

The imaging system was used as described previously [17]. Briefly, it was based on an inverted fluorescence microscope equipped with a 100 W mercury lamp and a Fluor 40×/1.30 oil objective (Axio observer D1, Carl Zeiss, Germany). Fluorescence signal was acquired by an electron multiplying charge-coupled device (DU-897D, Andor, UK). The MetaMorph software (Version 7.1, Universal Imaging Corp., USA) was used to control the acquisition and analyze the fluorescence data from individual cells. For Ca<sup>2+</sup> detection, cells incubated with Fluo-3 AM were excited at 485/20 nm, and fluorescence was collected with a 510 nm long-pass dichroic mirror and a 540/50 emission filter. For NAD(P)H autofluorescence imaging, cells were directly excited by a mercury lamp with a 365/50 excitation filter, and fluorescence was obtained with a 400 nm long-pass dichroic mirror and a 450/58 emission filter.

## 3. Results

### 3.1. Dependence on loading and de-esterification temperatures

Usual staining procedures for Fluo-3 AM, which are performed at temperatures in the range 15 °C <  $T_L$  < 37 °C and 20 °C <  $T_D$  < 37 °C tend to give darker nucleus than cytoplasm in the fluorescence images [18]. In our method, osteoblast cells were loaded with Fluo-3 AM for 20 min at  $T_L = 4, 20$ , and 37 °C, respectively. A subsequent de-esterification process took place for 30 min at  $T_D = 20$  or 37 °C. The resulting fluorescence images were shown

in Fig. 1. The green images correspond to Fluo-3 fluorescence and the blue ones indicate NAD(P)H autofluorescence. Because NAD(P)H is mostly distributed in cytoplasm [19], its autofluorescence imaging can clearly resolve the regions between nucleus and cytoplasm. From our results it was evident that cold loading ( $T_L = 4$  °C) and room temperature ( $T_D = 20$  °C) de-esterification result in a remarkably brighter nucleus than cytoplasm, which was indicated with red arrows in the upper-left image in Fig. 1A. Under these conditions, the mean relative fluorescent intensity (MRFI) from the nucleus was approximately twice as large as from the cytoplasm ( $17.4 \pm 5.3$  for nucleus vs.  $8.7 \pm 5.7$  for cytoplasm) as shown in Fig. 1B (a).

Furthermore, for the same de-esterification temperature ( $T_D = 20$  °C), room temperature ( $T_L = 20$  °C) loading gave slightly brighter nucleus, which were hard to be resolved in the fluorescence images (Fig. 1B (b)), while warm loading ( $T_L = 37$  °C) in general produced darker nucleus than the cytoplasm (Fig. 1B (c)). For de-esterification taking place at  $T_D = 37$  °C, osteoblast cells displayed darker nucleus than the cytoplasm, no matter what loading temperature  $T_L$  was used (Fig. 1B (d–f)). Taken together, Fluo-3 AM-incubated osteoblast cells exhibit brighter fluorescence in nucleus depending on the treatment of cold loading ( $T_L = 4$  °C) and room temperature de-esterification.

### 3.2. Dependence on loading time

In Fig. 1A, one could notice in the image up left that the nucleus appeared brighter than the surrounding cytoplasm, however the associated fluorescence intensity was quite low. For that reason, our next goal was to increase the average fluorescence intensity. It was natural to expect that longer loading time would lead to stronger fluorescence. Therefore, with keeping de-esterification temperature at  $T_D = 20$  °C, we loaded osteoblast cells with Fluo-3 AM at  $T_L = 4$  °C for 20 and 50 min, respectively. The results clearly demonstrated that longer loading time gave brighter nuclear fluorescence (Fig. 2A). Yet, the ratio of MRFI in the nucleus and in the cytoplasm stayed at the value of about 2 ( $28 \pm 2.4$  for nucleus vs.  $14 \pm 2.7$  for cytoplasm; Fig. 2A).

### 3.3. Dependence on adhesion quality

The next step was testing whether the above described method of cold loading ( $T_L = 4$  °C) and room temperature de-esterification ( $T_D = 20$  °C) worked the same in other cell types. First, HeLa cells, another kind of adherent cell, were selected to test the protocol. The corresponding images were shown in left images in Fig. 2B. Similar to that of osteoblasts, longer loading time induced stronger nuclear fluorescence in HeLa cells. Second, BV2 cells were used to further confirm the protocol. Interestingly, the protocol worked for strongly adherent BV2 cells (in the minority) with the polarized shape (whiter arrows in Fig. 2B), but it failed for weakly adherent cells (in the majority) that typically exhibited a spherical shape. For the weakly adherent BV2 cells, no distinct boundary between the nucleus and the cytoplasm could be resolved by our protocol. Similar properties were reported for suspension cells loading by Fura-2 AM [20].

To further resolve the effect of adherent status of the cells on the fluorescence intensity, we incubated osteoblast cells on glass cover slips just for 2 h before the experiments and then stained them via the above-described method ( $T_L = 4$  °C,  $T_D = 37$  °C). The results were shown in Fig. 3. The cells that were just weakly stuck to the cover slip surface and consequently exhibited a poor adherent status, displayed no clear border of the nucleus region in both: NAD(P)H and Fluo-3 fluorescence images (cell 1 and 2 in Fig. 3). However, if the cells were fully adherent, the area of nucleus became distinct and clear, with brighter fluorescence from the



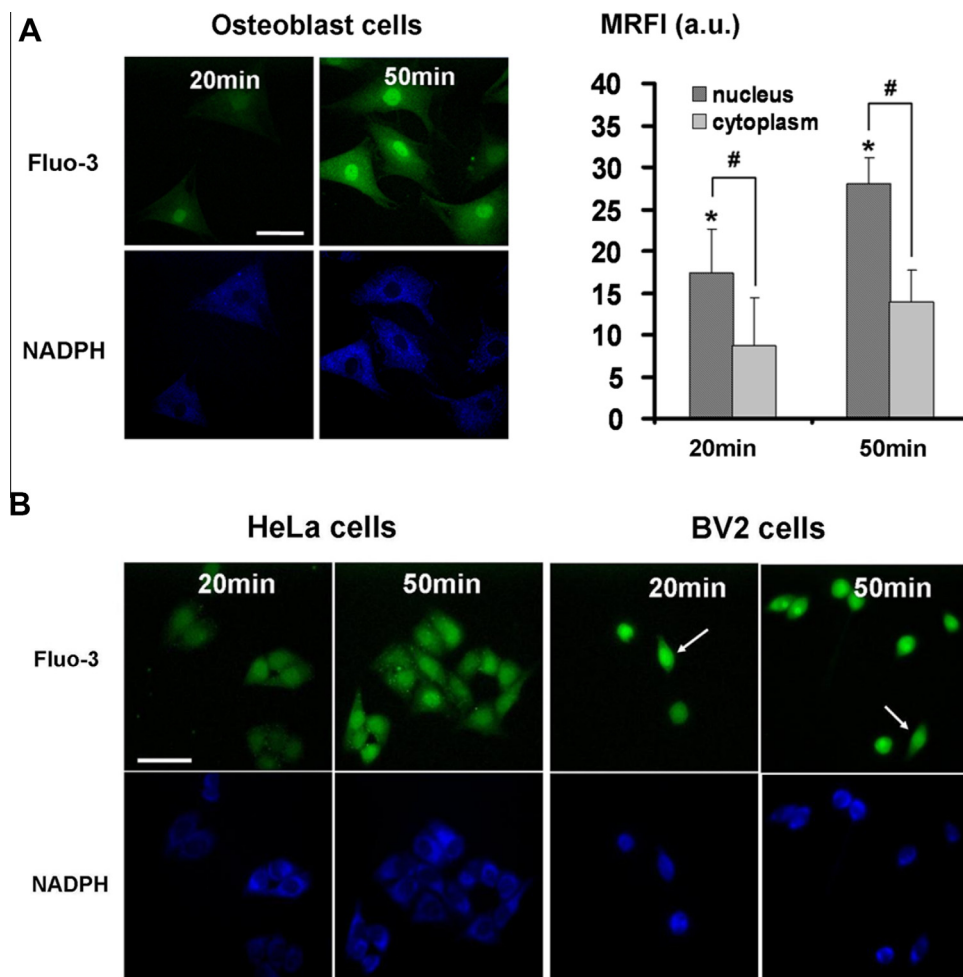


**Fig. 2.** Fluorescence data for osteoblast cells, HeLa cells and BV2 cells loaded by Fluo-3 AM at 4 °C and de-esterified at 20 °C. (A) Representative fluorescent images of osteoblast cells (left panes) and statistic data for MRFI from the nucleus and cytoplasm (right pane). All cells were loaded at  $T_L = 4$  °C for 20 and 50 min, respectively, and then de-esterified at  $T_D = 20$  °C for 30 min. The images of Fluo-3 (green) and NADPH(H) (blue) indicated that the longer the cold loading time, the brighter the nuclear fluorescence. Above 30 cells of each group were calculated from at least three repeated experiments ( $*P < 0.01$ , MRFI  $\pm$  SD). (B) Representative fluorescence images for HeLa cells and BV2 cells. HeLa cells (left panes) displayed the brighter fluorescence in nucleus than in cytoplasm, and longer loading time induced increasing of fluorescent intensities. However, for Bv2 cells (right panes), most of the images of Fluo-3 (green) and NADPH(H) (blue) exhibited no distinct boundary between nucleus and cytoplasm. The white arrows denote cells showing slightly brighter nucleus. All the experiments were repeated at least three times. Scale bar represents 50  $\mu$ m. (For interpretation of the references to color in this figure legend, the reader is referred to the web version of this article.)

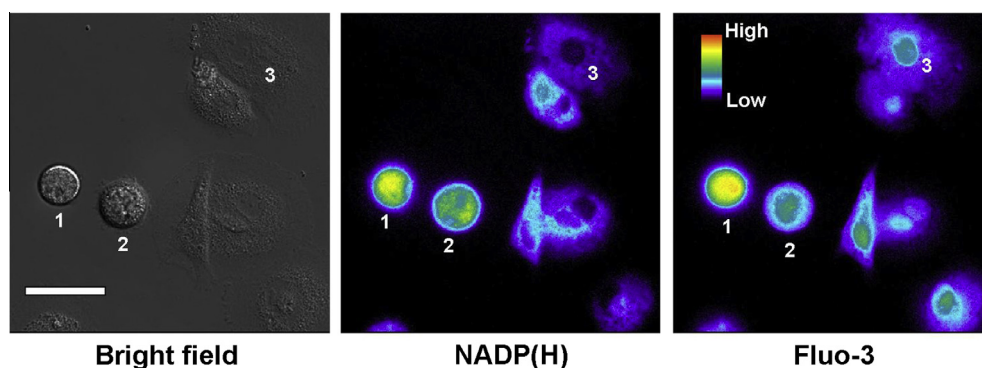


**Fig. 3.** Fluorescent images for osteoblast cells with different adherent status. (A) Bright field images. The adherent status for the cells labeled as 1, 2, and 3 was increasing from poor to good adhesion. (B) Pseudo color images of NADPH(H) fluorescence. No obvious border of the nucleus was evident for cell 1 and 2 (poor adhesion), while cell 3 (good adhesion) showed clear border. (C) Pseudo color images of Fluo-3 fluorescence. With increasing cell adherent status, the boundary between the nucleus and the cytoplasm became more evident (from cell 1 to 3). Scale bar represents 50  $\mu$ m. The color range was divided in the spectral sequence from high concentration (white) to low concentration (black). (For interpretation of the references to color in this figure legend, the reader is referred to the web version of this article.)

membrane, is temperature sensitive: they exhibit high activity at warm temperature ( $T = 37$  °C), low activity at room temperature

( $T = 20$  °C) and almost no activity at cold temperature ( $T = 4$  °C) [22]. OATs remove Fluo-3 from both nucleus and cytoplasm.



According to above-described arguments, we suggest that the low temperature loading at  $T_L = 4^\circ\text{C}$  allows free diffusion of Fluo-3 AM into cytoplasm and nucleus with rare cleavage of AM due to inactive esterase (Fig. 4A). A subsequent process of de-esterification at room temperature ( $T_D = 20^\circ\text{C}$ ) is efficient enough to induce Fluo-3 generation. On the other hand, room temperature is still low that most of the OATs are inactive. This combination results in equal densities of Fluo-3 in the nucleus and in the cytoplasm (Fig. 4D). Moreover, it was demonstrated [11] that  $[\text{Ca}^{2+}]_c$  and  $[\text{Ca}^{2+}]_n$  were almost same, while the fluorescence intensity of Fluo-3 in the nucleus was twice as large as in the cytoplasm. The difference is attributed to different fluorescent properties of Fluo-3 in the nucleus and in the cytoplasm. Therefore, for the same concentration of the  $\text{Ca}^{2+}$  in the nucleus and cytoplasm, the fluorescence intensity from the nucleus should be double that from the cytoplasm. This expectation was in very good agreement with our experimental results obtained for  $T_L = 4^\circ\text{C}$  and  $T_D = 20^\circ\text{C}$  as shown in Fig. 1B (a).

In the case of room temperature loading, parts of Fluo-3 AM are cleaved away before entering nucleus. This results in larger density of Fluo-3 in the cytoplasm with respect to nucleus (Fig. 4B). Meanwhile, the loss of Fluo-3 can be neglected due to the relatively low activity of OATs at room temperature (Fig. 4D). Under these conditions, the fluorescence intensity from the nucleus is only slightly larger than from the cytoplasm (Fig. 1B (b)).

However, warm temperature ( $T = 37^\circ\text{C}$ ) not only allows far more Fluo-3 trapped in cytoplasm than in nucleus because of the high activity of esterase (Fig. 4C), but also accelerates loss of Fluo-3 from nucleus and cytoplasm induced by activated OATs in pure HBSS (Fig. 4C and E). This transport reduces concentration of Fluo-3 in the nucleus as well as its concentration in the cytoplasm, and consequently in the fluorescence images the nucleus becomes darker than the cytoplasm (Fig. 1B (c–f)). In addition, free Fluo-3 can pass back to the nucleus through the nuclear pore complex via diffusion, but in reality the Fluo-3 diffusion between the cytoplasm and the nucleus is weak due to its high affinity to  $\text{Ca}^{2+}$  [23].

Such increase of fluorescence intensity of Fluo-3 from the nucleus region following our staining protocol ( $T_L = 4^\circ\text{C}$  and  $T_D = 20^\circ\text{C}$ ) could be proved also from the real-time measurements. We observed time-dependence increase of fluorescence intensity in the nucleus and the cytoplasm region during de-esterification process (data not shown). A low fluorescent intensity detected in the beginning of the de-esterification process suggested that cold loading only allowed Fluo-3-AM to freely diffuse into the cytoplasm and the nucleus, while the cleavage of the AM groups was rare. During the subsequent de-esterification, the AM groups were removed and the remaining Fluo-3 indicators started to emit fluorescent light.

Interestingly, it was known that cold shock and rewarming affected various cell physiological activities including protein

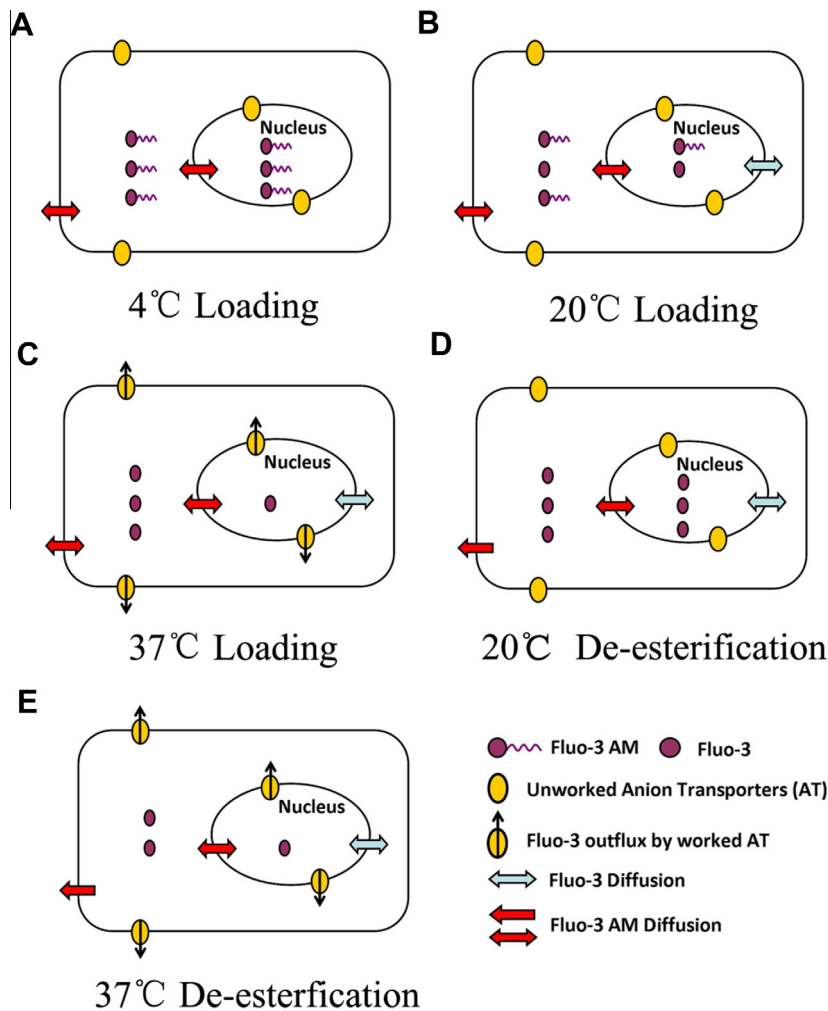


**Fig. 4.** Schematic drawings of different processes governing Fluo-3 AM and Fluo-3 distribution at different temperatures. When loading takes place at  $4^\circ\text{C}$ , Fluo-3 AM freely diffuses into cytoplasm and nucleus, while cleavages of the AM tail are rare (A). Esterase promotes trapping of Fluo-3 in the cytoplasm region, which becomes efficient at  $20^\circ\text{C}$  (B, D), and further increases at  $37^\circ\text{C}$  (C, E). Organic anion transporters located in the nuclear and plasma membranes are inactive at  $4^\circ\text{C}$  (A), moderately active at  $20^\circ\text{C}$  (B, D) and very active at  $37^\circ\text{C}$  (C, E).

synthesis [24], gene transcription [25], cell cycle [26], intracellular calcium [27] and so on. Thus, it is necessary to taken into account the effects of temperature shock on calcium signals for our experiments. Researchers demonstrated that the influences of cold shock and rewarming on cells usually occurred when temperature was higher than 37 °C, such as 42 °C, with time more than 1 h [25]. Furthermore, the rising of  $[Ca^{2+}]_n$  and  $[Ca^{2+}]_c$  induced by temperature shock could quickly recover to resting state within minutes [28,29]. Therefore, it seems likely that temperature shock might not be the critical factor for the results of brighter fluorescent nucleus shown in this work.

In addition, it was found that this new staining protocol only “worked” in cells with polarized shape in BV2 cells (denoted by white arrows in Fig. 2B). A polarized shape signifies good adherent status, while a spherical shape is characteristic for weak adhesion. In addition to this, we found that osteoblast cells with different adherent status used in experiments related to Fig. 3, also showed some adhesion dependent properties. The weakly attached cells displayed no clear boundary between the nucleus and cytoplasm areas (for both Fluo-3 and NADP(H) images), while the fully adherent ones showed a clear boundary. With increasing adhesion quality, the appearance of the boundary between the nucleus and the cytoplasm varied from blurred to distinct (cells 1, 2 and 3 in Fig. 3). Therefore, we concluded that loading at  $T_L = 4$  °C and de-esterification at  $T_D = 20$  °C could produce brighter nuclei only in well adherent cells.

In conclusion, the loading and de-esterification temperature play an important roles in Fluo-3-AM loading. Our study showed that the optimized loading conditions of Fluo-3-AM at  $T_L = 4$  °C loading, and at  $T_D = 20$  °C de-esterification resulted in the brighter nucleus in adherent cells. This optimized condition has no disadvantages of direct injection, including membrane perforation, cell damage, operation complexity, and long processing time. Besides, genetically encoded calcium indicators (GECIs) based on green fluorescent protein allow researcher to detect calcium dynamics in specific targeted locations, such as  $[Ca^{2+}]_n$ , with living cells [30], but it has an inherent deficiency with respect to fast transient calcium signals. As a mature probe, Fluo-3 AM is used easily and exhibit better temporal properties with a higher signal-to-noise ration than that of GECIs [31]. Therefore, our developed method may be more responsive to quickly and simultaneously detect  $[Ca^{2+}]_c$  and  $[Ca^{2+}]_n$ , which is beneficial to investigate the regulating roles of  $[Ca^{2+}]_n$  in adherent cells.

## Acknowledgments

This work was supported by the National Natural Science Foundation of China (No. 11204142), the National Basic Research Program of China (No. 2010CB934101), International S&T cooperation program of China (2011DFA52870), the Specialized Research Fund for the Doctoral Program of Higher Education (No. 20110031120004), the 111 Project (No. B07013), the National Natural Science Foundation of China (Nos. 11074133, 31160370) and the National Science Fund for Talent Training in Basic Sciences (No. J1103208).

## References

- [1] J. Alvarez, M. Montero, J. Garcia-Sancho, Subcellular  $Ca^{2+}$  dynamics, *News Physiol. Sci.* 14 (1999) 161–168.
- [2] M.T. Alonso, J. Garcia-Sancho, Nuclear  $Ca^{2+}$  signalling, *Cell Calcium* 49 (2011) 280–289.
- [3] M.D. Bootman, C. Fearnley, I. Smyrnias, F. MacDonald, H.L. Roderick, An update on nuclear calcium signalling, *J. Cell Sci.* 122 (2009) 2337–2350.
- [4] R.E. Dolmetsch, K. Xu, R.S. Lewis, Calcium oscillations increase the efficiency and specificity of gene expression, *Nature* 392 (1998) 933–936.
- [5] G. Bkaily, M. Nader, L. Avedanian, et al., G-protein-coupled receptors, channels, and  $Na^+H^+$  exchanger in nuclear membranes of heart, hepatic, vascular endothelial, and smooth muscle cells, *Can. J. Physiol. Pharmacol.* 84 (2006) 431–441.
- [6] M.F. Leite, E.C. Thrower, W. Echevarria, P. Koulen, K. Hirata, A.M. Bennett, B.E. Ehrlich, M.H. Nathanson, Nuclear and cytosolic calcium are regulated independently, *Proc. Natl. Acad. Sci. U.S.A.* 100 (2003) 2975–2980.
- [7] D.M. O'Malley, B.J. Burbach, P.R. Adams, Fluorescent calcium indicators: subcellular behavior and use in confocal imaging, *Methods Mol. Biol.* 122 (1999) 261–303.
- [8] N. Parkinson, S. Bolsover, W. Mason, Nuclear and cytosolic calcium changes in osteoclasts stimulated with ATP and integrin-binding peptide, *Cell Calcium* 24 (1998) 213–222.
- [9] D.M. O'Malley, Calcium permeability of the neuronal nuclear envelope: evaluation using confocal volumes and intracellular perfusion, *J. Neurosci.* 14 (1994) 5741–5758.
- [10] J.P.Y. Kao, A.T. Harootunian, R.Y. Tsien, Photochemically generated cytosolic calcium pulses and their detection by Fluo-3, *J. Biol. Chem.* 264 (1989) 8179–8184.
- [11] C. Perez-Terzic, L. Stehno-Bittel, D.E. Clapham, Nucleoplasmic and cytoplasmic differences in the fluorescence properties of the calcium indicator Fluo-3, *Cell Calcium* 21 (1997) 275–282.
- [12] M.W. Roe, J.J. Lemasters, B. Herman, Assessment of Fura-2 for measurements of cytosolic free calcium, *Cell Calcium* 11 (1990) 63–73.
- [13] S. Ljubojević, S. Walther, M. Asgarzoei, et al., In situ calibration of nucleoplasmic versus cytoplasmic  $Ca^{2+}$  concentration in adult cardiomyocytes, *Biophys. J.* 100 (2011) 2356–2366.
- [14] D.E. Clapham, Calcium signaling, *Cell* 80 (1995) 259–268.
- [15] D. Thomas, S.C. Tovey, T.J. Collins, M.D. Bootman, M.J. Berridge, P. Lipp, A comparison of fluorescent  $Ca^{2+}$  indicator properties and their use in measuring elementary and global  $Ca^{2+}$  signals, *Cell Calcium* 28 (2000) 213–223.
- [16] S. Kou, L. Pan, D.V. Noort, et al., A multishear microfluidic device for quantitative analysis of calcium dynamics in osteoblasts, *Biochem. Biophys. Res. Commun.* 408 (2011) 350–355.
- [17] L. Pan, X. Wu, D. Zhao, et al., Sulfhydryl modification induces calcium entry through  $IP_3$ -sensitive store-operated pathway in activation-dependent human neutrophils, *PLoS ONE* 6 (2011) e25262.
- [18] J.P.Y. Kao, Practical aspects of measuring  $[Ca^{2+}]_i$  with fluorescent indicators, *Methods Cell Biol.* 40 (1994) 155–181.
- [19] W. Ying,  $NAD^+/NADH$  and  $NADP^+/NADPH$  in cellular functions and cell death: regulation and biological consequences, *Antioxid. Redox Signal.* 10 (2008) 179–206.
- [20] A. Malgaroli, D. Milani, J. Meldolesi, T. Pozzan, Fura-2 measurement of cytosolic free  $Ca^{2+}$  in monolayers and suspensions of various types of animal cells, *J. Cell Biol.* 105 (1987) 2145–2155.
- [21] S.H. Hammer, C.D. Bishop, S.A. Watts, Activities of three digestive enzymes during development in the crayfish *Procambarus clarkii* (Decapoda), *J. Crustacean Biol.* 20 (2000) 614–620.
- [22] T.H. Steinberg, A.S. Newman, J.A. Swanson, Macrophages possess probenecid-inhibitable organic anion transporters that remove fluorescent dyes from the cytoplasmic matrix, *J. Cell Biol.* 105 (1987) 2695–2702.
- [23] D. Stoffler, K. Schwarz-Herion, U. Aebi, B. Fahrenkrog, Getting across the nuclear pore complex: new insights into nucleocytoplasmic transport, *Can. J. Physiol. Pharmacol.* 84 (2006) 499–507.
- [24] F.M. Underhill, C.M. Smales, The cold-shock response in mammalian cells: investigating the HeLa cell cold-shock proteome, *Cytotechnology* 53 (2007) 47–53.
- [25] J. Fujita, Cold shock response in mammalian cells, *J. Mol. Microbiol. Biotechnol.* 1 (1999) 243–255.
- [26] C.L. Rieder, R.W. Cole, Cold-shock and the mammalian cell cycle, *Cell Cycle* 1 (2002) 169–175.
- [27] G. Bellomo, M. Perotti, F. Taddei, et al., Tumor necrosis factor  $\alpha$  induces apoptosis in mammary adenocarcinoma cells by an increase in intranuclear free  $Ca^{2+}$  concentration and DNA fragmentation, *Cancer Res.* 52 (1992) 1342–1346.
- [28] H. Knight, M.C. Knight, Imaging spatial and cellular characteristics of low temperature calcium signature after cold acclimation in Arabidopsis, *J. Exp. Bot.* 51 (2000) 1679–1686.
- [29] I.T. Aznar, F. Leganés, I. Bonilla, F. Fernández-Piñas, Use of recombinant aequorin to study calcium homeostasis and monitor calcium transients in response to heat and cold shock in cyanobacteria, *Plant Physiol.* 123 (2000) 161–175.
- [30] M. Whitaker, Genetically-encoded probes for measurement of intracellular calcium, *Methods Cell Biol.* 99 (2010) 153–182.
- [31] M. Carter, J.C. Shieh, Visualizing nervous system function, in: M. Carter, J.C. Shieh (Eds.), *Guide to Research Techniques in Neuroscience*, Elsevier Inc., Canada, 2010, pp. 169–189.